Available online at BCREC website: https://bcrec.id

Bulletin of Chemical Reaction Engineering & Catalysis, 18 (2) 2023, 186-199

Research Article

Studies of the Solvent-Free Knoevenagel Condensation over Commercial NiO compared with NiO Drived from Hydrotalcites

Nadia Aider[1,4,*], Baya Djebarri[2,4], Fouzia Touahra[3,4,*], Hatem Layeb[1], Djamila Halliche[4]

[1]*Laboratoire de Chimie Appliquée et de Génie Chimique (LCAGC), Université Mouloud Mammeri, 15000, Tizi-Ouzou, Algeria.*
[2]*Laboratory of Applied Chemistry and Materials (LabCAM), University of M'hamed Bougara of Boumerdes, Avenue de l'Indépendance Boumerdes, 35000. Algeria.*
[3]*Centre de Recherche Scientifique et Technique en Analyses Physico-chimiques (CRAPC), BP 384-Bou-Ismail,RP42004, Tipaza, Algeria.*
[4]*Laboratoire de Chimie du Gaz Naturel Faculté de Chimie, Université des Sciences et de la Technologie Houari Boumediène, BP 32 El-Alia, 16111, Bab-Ezzouar, Alger, Algeria.*

Received: 5th March 2023; Revised: 3rd May 2023; Accepted: 4th May 2023
Available online: 6th May 2023; Published regularly: July 2023

Abstract

In this study, we compared the effect of the commercial NiO, synthesis NiAl-HT and NiO-HT drived from hydrotalcite in Knoevenagel condensation reaction. The NiAl-HT sample was synthesized by the coprecipitation method with a molar ratio M^{2+}/M^{3+} = 2 at constant basic pH. X-ray Diffraction (XRD) and Fourier Transform Infrared Spectroscopy (FTIR) were utilized to identify crystalline phases present in NiAl-HT, NiO-HT and commercial NiO. The chemical composition of the obtained solids was determined by Atomic Absorption Spectroscopy (AAS). Other techniques, such as Thermogravimetric Thermal Analyzer (TGA), Scanning Electron Microscopy (SEM) and Brunauere Emmette Teller Method (BET) were also used. As well as the BET showed the increase of the specific surface for the solid NiO-HT. The performance of the catalysts were studied in Knoevenagel condensation of benzaldehyde with ethyl acetoacetate without solvent to synthesis of organic compounds such as intermediates of dihydropyridines derivatives. The influence of different parameters, such as: catalyst amount, reaction temperature and reaction time, were optimized for studied the activity, the selectivity and the stability of the solids. Catalytic activity was in its lowest in the presence of NiAl-HT (26% of benzaldehyde conversion) whereas the benzaldehyde conversion increased to 77% in case of NiO-HT which can be explained by the presence of the basic sites of the NiO-HT oxides, a high surface area and a small crystallite size. Therefore, the lower increase in benzaldehyde conversion was noticed using commercial NiO (84%), perhaps owing to its high purity. A reaction mechanism is proposed by using density functional method (DFT).

Keywords: NiO-HT; Commercial NiO; Knoevenagel reaction; Density functional theory (DFT)

How to Cite: N. Aider, B. Djebarri, F. Touahra, H. Layeb, D. Halliche (2023). Studies of the Solvent-Free Knoevenagel Condensation over Commercial NiO compared with NiO Drived from Hydrotalcites. *Bulletin of Chemical Reaction Engineering & Catalysis*, 18(2), 186-199 (doi: 10.9767/bcrec.17598)

Permalink/DOI: https://doi.org/10.9767/bcrec.17598

1. Introduction

The Knoevenagel condensation is a carbon-carbon bond-forming (C=C bond) reaction between aldehydes or ketones and an activated methylene compound (e.g. malononitrile or ethyl cyanoacetate) [1,2]. This reaction has been used to produce of α,β-unsaturated like esters, acids and nitriles, widely used as intermediates in the synthesis of pharmaceuticals product, cosmetic,

* Corresponding Author.
Email: tfafaze256@yahoo.fr (F. Touahra);
nadia.aider@ummto.dz (N. Aider);

agrochemicals, and natural products [2–4]. Generally this reaction is catalyzed by organo-bases, such as ammonia, primary and secondary amines, quaternary ammonium salts, piperidine or pyridine, which deprotonates the methylene compound and activates it towards nucleophilic attack by the carbonyl group of the aldehyde or ketone [1,2]. But using these homogeneous base catalysts often leads to time consuming work-up procedures, and undesired side-reactions. The literature mentions, that the use of strong acid catalysts causes waste removal problem and recovery of the catalyst from the reaction [5], and also reported that Lewis acid catalysts known for Knoevenagel condensation are limited compared to bases as catalysts. Some of Lewis acid catalysts used for Knoevenagel condensation under solvent-free conditions, such as $Mg(ClO_4)_2$ [6], CuCl [7] , $LaCl_3$ [8], $ZnCl_2$ [9], and $SnCl_4$ [10], need to be used in more than stoichiometric quantity which causes waste disposal problem. Furthermore, Lewis acid catalysts are extremely moisture-sensitive thereby demanding keeps moisture-free reaction conditions [11,12].

Recently, the acid-base catalysts easily separable and reusable were used for the Knoevenagel condensation reactions such as zeolites [13] hydrotalcite [14] and sulfonic acid [15]. Among based-catalysts very used in Knoevenagel condensation of benzaldehyde reaction, hydrotalcite due to its advantages, over the solid acid catalysts [12], and they can be doped to give a higher activity and a better selectivity [16–18]. Most of these catalysts have been used to catalyze the Knoevenagel condensation in the presence of solvents. The metal oxides derived from hydrotalcite can act as bases to absorb the strongly acidic protons from an active methylene bearing organic compound, which generate carbanions without solvent [12].

Hydrotalcite-type (HT) compounds had many practical applications as catalysts or catalyst precursors or supports [19], ion exchangers [20], stabilizers and adsorbents [21,22]. In particular, the mixed oxide obtained of HT precursors presented high surface area, basic properties and small crystal sizes. These compounds have the general formula: $[M^{2+}_{1-x}M^{3+}_x(OH)_2][A^{n-}]_{x/n}.yH_2O$, where M^{2+} and M^{3+} are di- and trivalent metal cations, respectively, *A* represents the *x* valent anion, which is needed to compensate the net positive charge of the brucite-like layers and *y* is the number of water molecules in the interlayer space [23]. For all these properties, the synthesis of these products has provided our attention to used these catalysts for catalyze the Knoevenagel condensation under solvent-free conditions.

Devi *et al.* [24] have found that KOH-loaded MgAl studied the effect of base precursors on the structure and basicity of the host employed for the Knoevenagel condensation reaction efficiently giving 99% conversion and 100% selectivity within 10 min. Mancipe *et al.* [25] studied the applicability of boric acid deposited on hydrotalcite as a catalyst in the Knoevenagel reaction of HMF derivatives and active methylene compounds to give new HMF derivatives containing an acrylonitrile moiety under solvent-free conditions. Jadhav *et al.* [26] synthesized Ti-HT and Zn-HT using glycine and glycerol as two different fuels in the method of synthesis by combustion which have been applied in the Knoevenagel condensation. The Ti-HT-glycine was the most active and selective. It gave 67% benzaldehyde conversion in 4 h at 60 °C. HT compounds were considered as suitable precursors of nickel catalysts [27,28], allowing homogeneous distribution of nickel inside the structure of the precursors and then leading to the well dispersed and stable metal nickel particles.

The thermal decomposition of NiAl-HT hydrotalcite at about 450 °C gives rise to mixed oxides whose X-ray diffraction patterns indicate a diffuse $Ni(Al)O_x$ periclase-type structure with no segregate crystalline phases [29,30]. The catalytic application of mixed oxides obtained from hydrotalcite NiAl-HT include base-catalyzed reactions, such as aldolic condensation, the cross-aldol condensation of aldehydes and ketones, Knoevenagel condensation, Claisen-Schmidt condensation, and Michael addition [31–35]. Recently, a group of researchers worked extensively on nickel oxide which has interesting physico-chemical properties which they then used in various biomedical applications [36]. Baranwal *et al.* [37] also showed that Cu-doped NiO nanoparticles are excellent catalysts for organic syntheses.

The main objective of this work is to compare the performance of the pure NiO commercial with the NiO-HT obtained from hydrotalcite by thermal treatment of NiAl-HT at 450 °C, in the Knoevenagel condensation of benzaldehyde reaction without solvents (Scheme 1). The comparison is likely to involve various aspects, including the yield of the desired product, the selectivity towards the desired product, and the reaction rate.

2. Materials and Methods

2.1 Raw Materials

The compounds used as starting materials in the synthesis of NiAl-HT were, $Al(NO_3)_3.9H_2O$ (Sigma-Aldrich®, 99.99%), $Ni(NO_3)_2.6H_2O$ (Sigma-Aldrich®, 99.99%) and Na_2CO_3 (Panreac, 98% assay) and NaOH (Sigma-Aldrich®, ≥98%). The commercial nickel oxide NiO were also supplied by Sigma-Aldrich® of high purity (99.99%), its density is 4.5 g/cm^3, the melting temperature is 1955 °C its bulk density is 600 kg/m^3.

2.2 Catalysts Synthesis

NiAl-HT was synthesized from the nitrates of Ni^{2+} and Al^{3+} with a molar ratio Ni^{2+}/Al^{3+} = 2 at constant pH (10±0.1), as reported by Touahra *et al*. [23]. Briefly, $Ni(NO_3)_2.6H_2O$ (0.50 M) and $Al(NO_3)_3.9H_2O$ (0.25 M) were dissolved in 100 mL of deionized water and second solution was prepared by dissolving NaOH and Na_2CO_3 in 100 mL of water. Both solutions were mixed dropwise under stirring at 25 °C. After the addition is complete, the mixture was aged at 80 °C for 15 h under vigorous stirring. Finally, the solid obtained was filtered and washed with distilled water, then that was dried and ground into a fine. The sample was calcined under air from room temperature up to 450 °C (5 °C.min^{-1}) for 6 h to produce the mixed oxides named NiO-HT.

2.3 Sample Characterization

Thermogravimetric analysis (TG) was performed using Thermal Analyzer Setaram Set Sys 16/18 from 25 to 900 °C with a heating rate of 10 °C/min in the presence of air. The chemical composition of each material was determined using atomic absorption spectroscopy (AAS) Varian spectra AA-110. The dissolution of solids was affected in the presence of nitric acid. The specific surface area of samples and pore size distribution calculations were determined by nitrogen adsorption using standard BET and BJH methods. Adsorption isotherms of nitrogen at −196 °C under study were recorded using a static volumetric apparatus ASAP 2020 (Micromeritics). The structure of samples were confirmed by X-ray powder diffraction with a Seifert C-3000 diffractometer with filtered Cu-Kα (λ = 1.5418 Å). The crystallites size for NiAl-HT, NiO-HT and commercial NiO solids were estimated using the Debey-Scherer equation [23]:

$$D_{hkl} = \frac{0.9\lambda}{\beta_{hkl}\cos\theta} \quad (1)$$

where, D_{hkl}= crystallites size, λ = wavelength of CuKα, β_{hkl} = peak with half maximum and θ is the Bragg diffraction angle.

FTIR spectra were recorded with Alpha Bruker (single reflection diamond ATR) spectrometer in the region 400–4000 cm^{-1}. The morphologies of the samples were studied using a Quanta 250 with tungsten filament scanning electron microscope (SEM).

2.4 Knoevenagel Condensation

The condensation of benzaldehyde (1) with ethyl acetoacetate (2) has been studied. An equimolecular solution of two reagents (14 mmol) was introduced into a two-necked 250 ml bottle, in the absence of solvent. The mixture is maintained in a thermostatically controlled silicone bath with magnetic stirring at a temperature of 80 °C. After 5 min of reaction, a mass of 0.50 g of catalyst was added to the mixture: this is the start of the reaction. Samples are taken every 30 min for 5 h with a syringe fitted with a filter, which makes it possible to separate the solid catalyst from the reaction products. Monitoring of the reaction is carried out by layer thin chromatography (TLC) and the revelation of the spots is carried out with iodine vapors and the color of these spots was yellow.

After each sample was reacted, the product was separated by transferring the hot reaction mixture to an ice bath and stirring for 5-10 min, and then filtered. The product is recovered by filtration and recrystallized using ethanol. The benzaldehyde conversion (X%) was calculated using the following equation [38]:

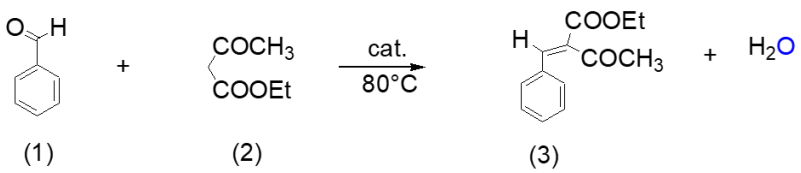

Scheme 1. Condensation of Benzaldehyde (1) with ethyl acetoacetate (2) in the Knoevenagel reaction.

$$X(\%) = \frac{Weight\ of\ benzaldehyde\ consumed\ (g)}{Initial\ weight\ of\ benzaldehyde\ (g)} \times 100 \quad (2)$$

2.5 Theoretical Calculations

DFT computations were carried out using the B3LYP Hybrid functional [39], together with the 6-31G (d.p.) basis set [40]. Optimizations were carried out using the Berny analytical gradient optimization method [41,42]. The stationary points were characterized by frequency computations in order to verify that the TSs have one and only one imaginary frequency. All computations were carried out with the Gaussian 09 suite of programs [43], and the results were visualized in GaussView [44].

3. Results and Discussion

3.1 Thermogravimetric Analysis (TG/DTG)

The data of TG-DTG, recorded in a temperature range of 25-1000 °C, with a speed of 10 °C/min, make it possible to follow the evolution of the structure as a function of the temperature and to determine the amount of structural water of each hydrotalcite type catalyst. The TG and DTG curves of the NiAl-HT sample is given in Figure 1. TGA values of analyzed sample is shown in Table 1. According to the literature [45], the thermal evolution of hydrotalcite solid in the carbonate form present, three well-defined weight losses. The first mass loss corresponds to the departure of molecules from physisorbed water (moisture water) on the external surface of the crystallites and the loss of inter-lamellar water without loss of structure [46]. A second mass loss at around 250 °C is due to dehydroxylation and the elimination of nitrates. The last loss of mass is characteristic of the departure of carbonates in CO_2 form [47].

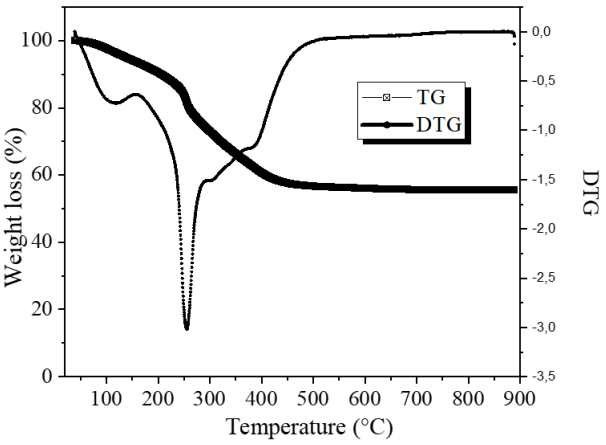

Figure 1. TG Analysis of NiAl-HT hydrotalcite.

3.2 Chemical Analysis

The chemical analysis of the uncalcined sample NiAl-HT was carried out by atomic absorption (AAS), after attack of the solid by HNO_3. This method of analysis makes it possible to give us the content of each constituent element of the catalyst and to arrive at its chemical formulation. Table 2 summarizes the results of the chemical analysis. It emerges from a Table 2 that the molar ratio Ni^{2+}/Al^{3+} is in agreement with the theoretical value. This confirms that precipitation of the precursor salts is taking place and shows the good operating conditions for the preparation of the catalyst.

Table 1. TG results of NiAl-HT hydrotalcite.

Sample	First weight loss (%)	Temperature (°C)	Second weight loss (%)	Temperature (°C)	Third weight loss (%)	Temperature (°C)
NiAl-HT	20	117	25	253	-	-

Table 2. The experimental molar ratio as well as the chemical formula of NiAl-HT, BET surface, total pore volume, pore diameter and crystalline size.

Samples	Molar ratios $R = \left[\frac{nM^{2+}}{nM^{3+}}\right]$	Chemical formulas $[M^{2+}_{(1-x)}M^{3+}_{x}]$	S_{BET} (m^2/g)	Total pore volume (cm^3/g)	Pore diameter (nm)	Crystalline size[a] (nm)
NiAl-HT	2.12	$Ni_{0.68}Al_{0.32}$	65.48	0.31	10-12	28
NiO-HT	-	-	82.30	0.28	7-8	14
Commercial NiO	-	-	83.78	0.27	7-8	20

[a]Crystalline size calculated from the XRD results in Figure 3.

3.3 Measurement of Specific Surface Areas

Table 2 represents the data calculated from the nitrogen adsorption/desorption at −196 °C. The specific surface area of NiAl-HT is 65.48 m^2/g. The heat treatment of NiAl-HT at 450 °C for 6 h caused an increase of the specific surface from 65.48 m^2/g to 82.78 m^2/g. This result can be explained by the fact that during the calcination step, the solids undergo degassing phenomena of the molecules of H_2O and of CO_3^{2-} (in CO_2 form) which are found in the pores on the surface of materials. The specific surface area of commercial NiO (83.78 m^2/g) is similar to that of NiO-HT.

Examination of the pore volume values in all the catalysts vary between 0.27 and 0.31 cm^3/g as well as their average pore diameters are between 7 and 12 nm (Table 2), which confirms that all the pores of the catalysts are of the mesoporous type. This result once again confirms that the mixed oxides phases from hydrotalcites are mesoporous materials (Figure 2).

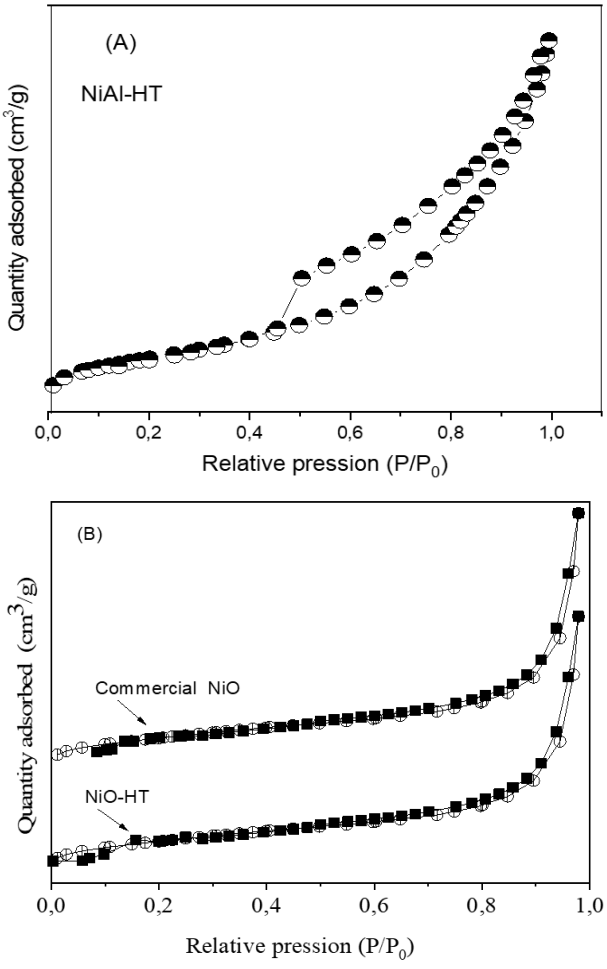

Figure 2. The nitrogen adsorption-desorption isotherm for samples (A) NiAl-HT hydrotalcite, (B) NiO-HT and commercial NiO.

3.4 X-ray Diffraction Analysis

The X-ray diffractogram of the uncalcined NiAl-HT, NiO-HT and commercial NiO samples was shown in Figure 3. In accordance with JCPDS file No. 15-0087, the X-ray diffractogram of the uncalcined sample is characterized by the presence of diffraction lines of the hydrotalcite phase. The latter crystallizes in a hexagonal mesh with principal reflections of the reticular planes (003), (006), (012), (015), (018) and (110) which correspond respectively to the angles of diffraction 2θ = 11.6°, 23.5°, 35.3°, 39.7°, 47.2°, 61.4°, and 62.8°. The calcination of sample at 450 °C leads to their dehydration ($-H_2O$) then to dehydroxylation and decarboxylation ($-CO_3^{2-}$) which is accompanied by the collapse of the HT structure. The calcination of NiAl-HT catalyst exhibited NiO diffraction peaks at 2θ = 37.2°, 43.2°, and 62.8° NiO [JCPDS file No. 47-1049]. These peaks, were relatively wide, indicating that it had a poor crystallinity. Aluminum oxide Al_2O_3 is in an amorphous state [48], therefore not detectable by X-ray diffraction. The solid diffractogram of the commercial NiO shows a pure peaks of NiO. The diffraction peak for the commercial NiO was sharp, indicating that it had a high crystallinity. Additionally, no other impurity peaks were observed, which shows that it had a higher purity.

3.5 SEM Analysis

The SEM images for the different solids are presented in Figure 4. In all cases, these images highlight platelet-shaped morphologies, which implies the formation of a lamellar structure of almost hexagonal shape. We can

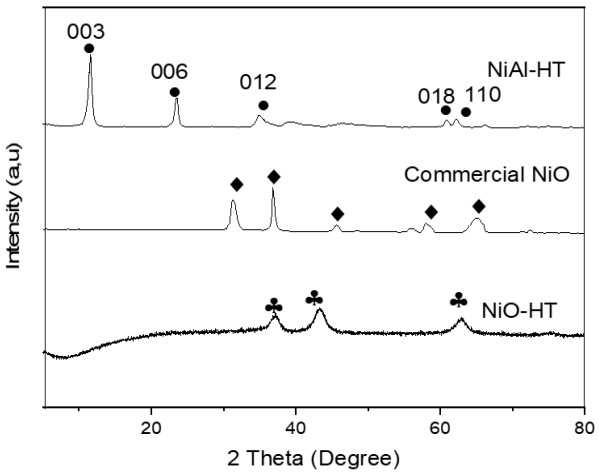

Figure 3. XRD patterns of NiAl-HT hydrotalcite, NiO-HT and commercial NiO. ● hydrotalcite, ♦ NiO and ♣ NiO-HT.

notice that the calcination of NiO-HT solid leads to the disappearance of the hexagonal shape and which has the same morphology as commercial NiO.

3.6 FTIR Analysis

The infrared spectra of the NiAl-HT, NiO-HT and commercial NiO samples are shown in Figure 5. IR spectra forum NiAl-HT present a wide adsorption band between 3500-3300 cm^{-1} attributed to the stretching vibrations of hydroxyl groups of water in the interlayer space [49]. Furthermore, the vibration band observed in the region between 1400–1500 cm^{-1} reveals the presence of O–C–O vibration of CO_3^{2-} in the interlayer space as reported in the literature [50]. We also observed low intensity vibration bands in the region below 1000 cm^{-1} which are associated to M^{2+}–O–M^{3+} (Ni–O–Al) stretching mode according to the literature [51]. After calcination the NiO-HT thermal decomposition of samples, induced formation of mixed oxides although trace amounts of remaining carbonate was found in the spectra of all calcined samples (band at 1320 cm^{-1}). Although absorption bands at 3370 and 1610 cm^{-1} (present in all spectra) indicate the presence of OH^- and/or water, we should recall that dehydroxylation of samples is complete at applied calcinations temperature (400–450 °C).

Commercial NiO spectra show peaks in region below 1000 cm^{-1} due to stretching vibrational peak of Ni–O bond. The absorption band at 1320 cm^{-1} is due to the stretching mode of O–C–O vibrations of CO_2 molecule absorbed from the air. The broad band at high frequency, *i.e.* around 3370 cm^{-1}, is attributed to –OH stretching vibrations of water molecules absorbed on catalyst surface from the atmosphere when analysis was carried out [52]. On the other hand, we observe the appearance of a new more or less intense band around 720 cm^{-1}. This band may indicate the probable formation of mixed oxides [53]. The calcined NiO-HT sample spectrum shape is similar to that of commercial NiO.

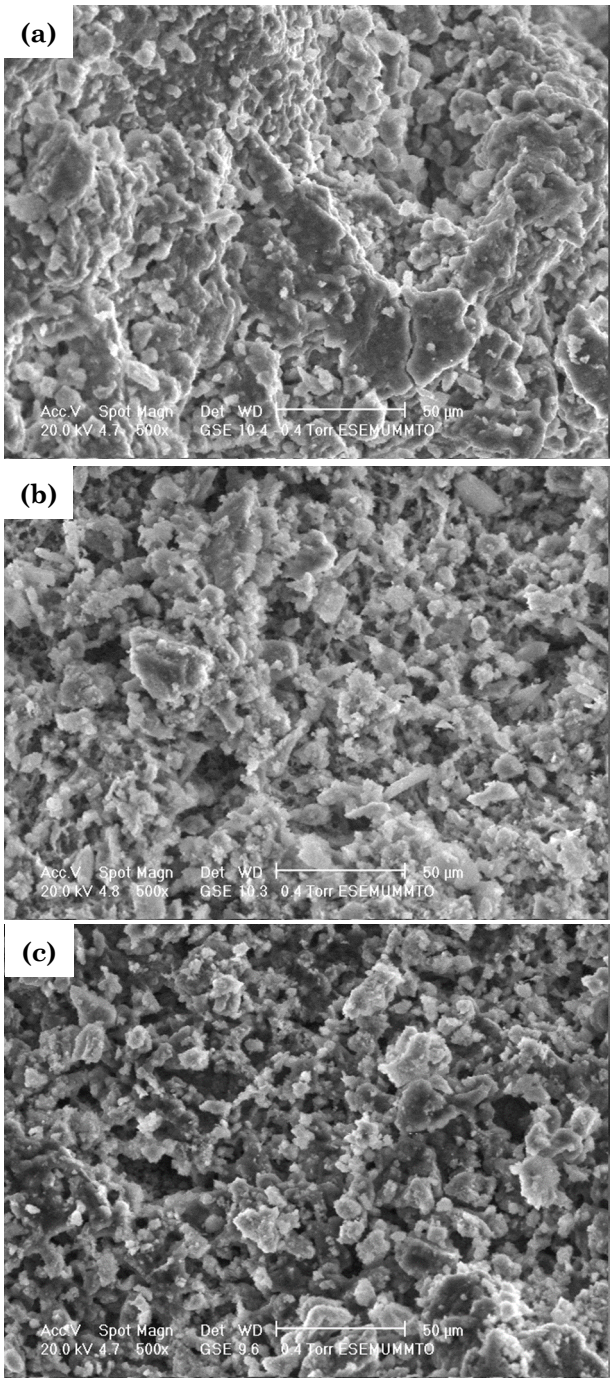

Figure 4. SEM images of samples: (a) NiAl-HT hydrotalcite, (b) NiO-HT and (c) commercial NiO.

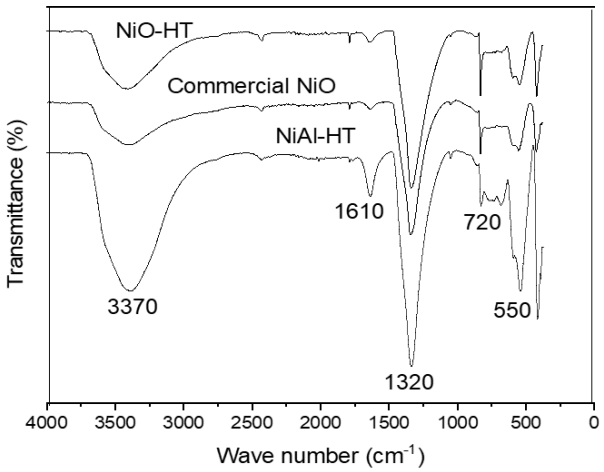

Figure 5. FTIR spectra of NiAl-HT hydrotalcite, NiO-HT and commercial NiO.

3.2 Catalytic Tests

3.2.1 Effect of reaction time

Figure 6 shows the results of the conversion of benzaldehyde with ethyl acetoacetate as a function of reaction time. In the absence of catalyst, the Knoevenagel condensation reaction does not occur, even after 4 h of reaction. In the presence of the catalysts, the conversion of the benzaldehyde reaches 26%, 77% and 84% after 3 h of reaction respectively of NiAl-HT, NiO-HT and commercial NiO. The NiAl-HT showed lower catalytic performance than commercial NiO and NiO-HT under the same reaction conditions. This result is explained by the lower specific surface of NiAl-HT (65 m^2/g). The increase in conversion obtained for the NiO-HT compared to NiAl-HT catalyst is justified by the strength of the basic sites of the oxides which should easily release the proton from ethyl acetoacetate to lead to the formation of the enolate anion, (see the reaction mechanism Scheme 4) high specific surface verified by BET analysis and a small crystallite size (Table 2)

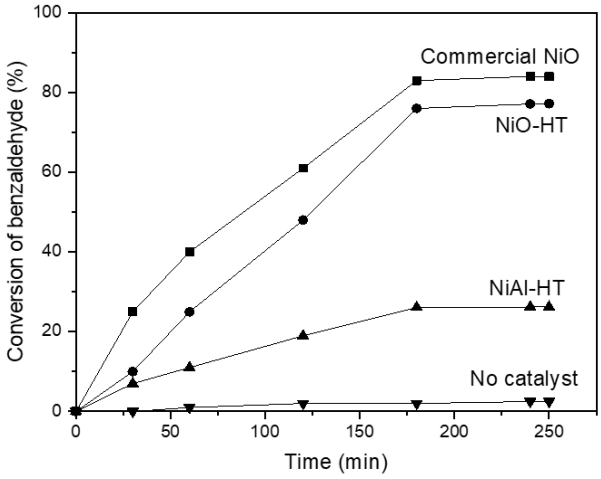

Figure 6. Conversion of benzaldehyde (1) in the Knoevenagel reaction as a function of time. Reaction conditions: benzaldehyde (1) (14 mmol) and ethyl acetoacetate (2) (14 mmol) and catalyst (0.50 g), at 80 °C.

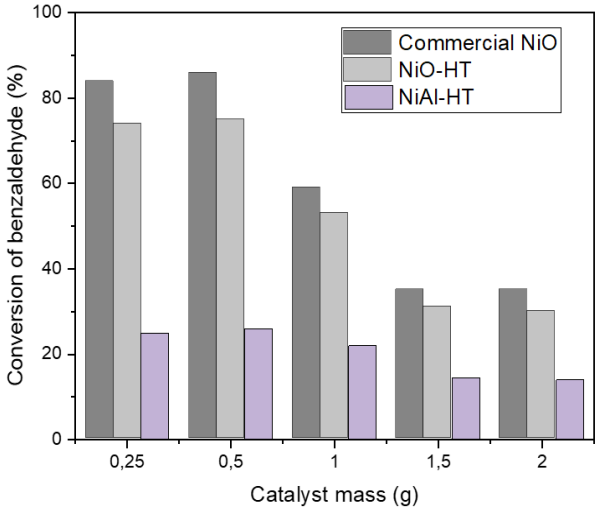

Figure 7. Effect of catalyst amount on conversion of benzaldehyde (1). Reaction conditions: benzaldehyde (1) (14 mmol) and ethyl acetoacetate (2) (14 mmol) and catalyst 0.50 g, at 80 °C.

The conversion rate of commercial NiO is lower increase than that of NiO-HT. This difference in conversion can be explained by high purity knowing that it is synthesized under ideal conditions on an industrial scale as previously observed in XRD (see Figure 3) [54].These results are in agreement with Chaudhary's *et al.* [55] study. This showed in the synthesis of 2oxoindolin3ylidenemalononitrile by Knoevenagel condensation in the presence of NiO catalyst under solvent-free conditions that the reaction gave excellent yield and environmental friendliness.

3.2.2 Effect of catalyst amount

The conversion of benzaldehyde is practically stable at 84% and 86% when the quantity of the catalyst passes from 0.25 g to 0.50 g (Figure 7). Increasing the amount of catalyst beyond 0.50 g leads to a gradual decrease in yield, it thus reaches 14% for an amount of 2 g of catalyst. This decrease would be linked either to the crowding of the active sites of the catalyst, given that the mass of the latter is high and/or to an inhibitory effect, always

Table 3. Total energies and relative energies of the reactants in the gas phase in the presence of catalyst.

	E (a.u.)	Δ*E* (kcal/mol)
R1	-345.58268	
R2	-460.35737	
NIO	-1583.1961	
R1+R2+NiO	-2389.1361	
NiOH	-1583.5484	
I2	-805.37981	
I2+NIOH	-2388.9282	130.43
I4	-805.9432	
I4+NiO	-2389.1393	-1.97
I3	-805.39532	
I3+NiOH	-2388.9438	120.70
P-trans	-729.50416	
P-cis	-729.50303	
P-trans+NiO+H_2O	-2389.1199	10.13
P-cis+NiO+H_2O	-2389.1188	10.84

linked to this excess by the formation of hydrogen bonds between the catalyst and the reactants [56,57]. In all case, working with large quantities of the catalyst switches the reaction from the catalytic mode to the stoichiometric mode, which is in disagreement with the standards of green chemistry. The best conversions of benzaldehyde are obtained in the presence of the commercial NiO catalyst.

3.2.3 Effect of reaction temperature

To optimize the experimental conditions, we then examined the effect of temperature on this reaction. Figure 8 shows the influence of the reaction temperature on the catalytic performance of commercial NiO and NiO-HT at 30, 60, 80, 100, and 120 °C for 4 h of reaction. At low temperature, no catalytic activity was shown, while at 60 °C and 80 °C, the conversion of benzaldehyde amounts to 51% and 86% respectively for commercial NiO and 38% and 71% for NiO-HT, respectively. Beyond this temperature (100 °C and 120 °C) a significant drop in the conversion is observed for the two catalysts. Following the appearance of several spots on the chromatogram of the analysis by thin layer chromatography, TLC, these spots can be explained by the appearance of unidentified secondary products.

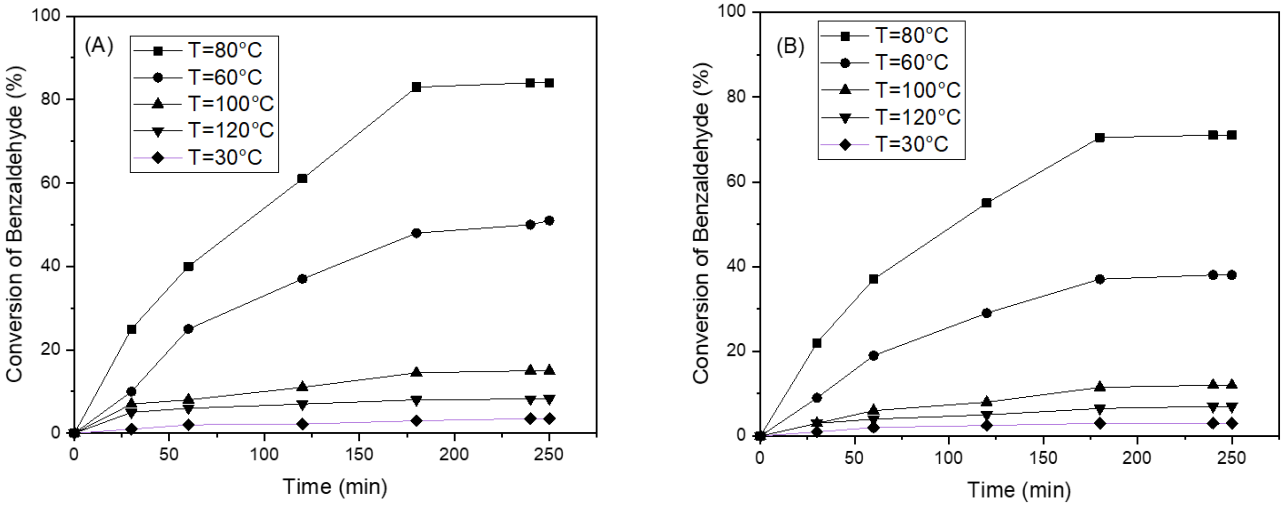

Figure 8. Effect of reaction temperature on conversion of benzaldehyde (1)of samples: (A) commercial NiO and (B) NiO-HT. Reaction conditions: benzaldehyde (1) (14 mmol) and ethyl acetoacetate (2) (14 mmol) and catalyst 0.50 g.

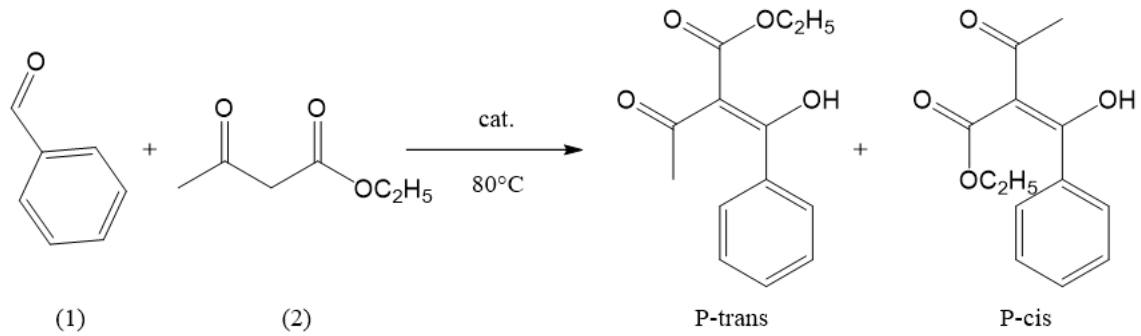

Scheme 2. Condensation of benzaldehyde (1)with ethyl acetoacetate (2).

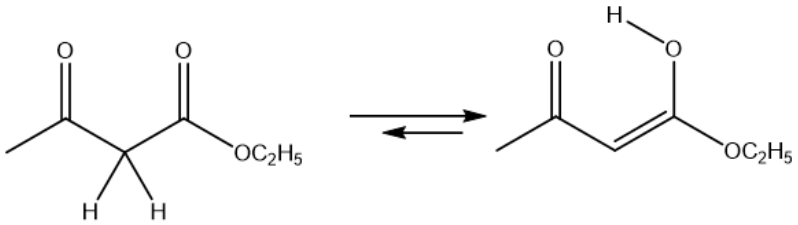

Scheme 3. The enol form of ethyl acetoacetate.

3.3 Reaction Mechanism

Due to the asymmetry of ethyl acetoacetate (2), the reaction between benzaldehyde (1) and ethyl acetoacetate (2) can occur via two possible stereo isomeric approaches, resulting in the formation of two potential cis and trans products (Scheme 2). The formation of these different products is linked to several intermediates. It should be noted that ethyl acetoacetate exists in the enol form with a concentration ranging from 1-5% in polar solvents and from 15 to 30% in nonpolar solvents from 15 to 30% (see Scheme 3). As a model, NiO was chosen as the catalyst in this study, and the proposed mechanism is illustrated in Scheme 4. Table 3 shows the total and relative energies of the reactants in the gas phase, while the geometries of the reactants and intermediates are presented in Scheme 5.

According to the obtained results, the relative energies of intermediates I2, I4, and I3 are 130.43, −1.97, and 120.70 kcal/mol, respectively. It is observed that the relative energies of intermediates I2 and I4 are very high, which can be explained by the presence of negative electronic charges on these intermediates. On the other hand, the relative energies of the P-trans and P-cis products are around 10.13 and 10.84 kcal/mol, respectively. Therefore, the P-trans product is more favorable than the P-cis product. In conclusion, the formation of the P-trans product is favored in the presence of the catalyst.

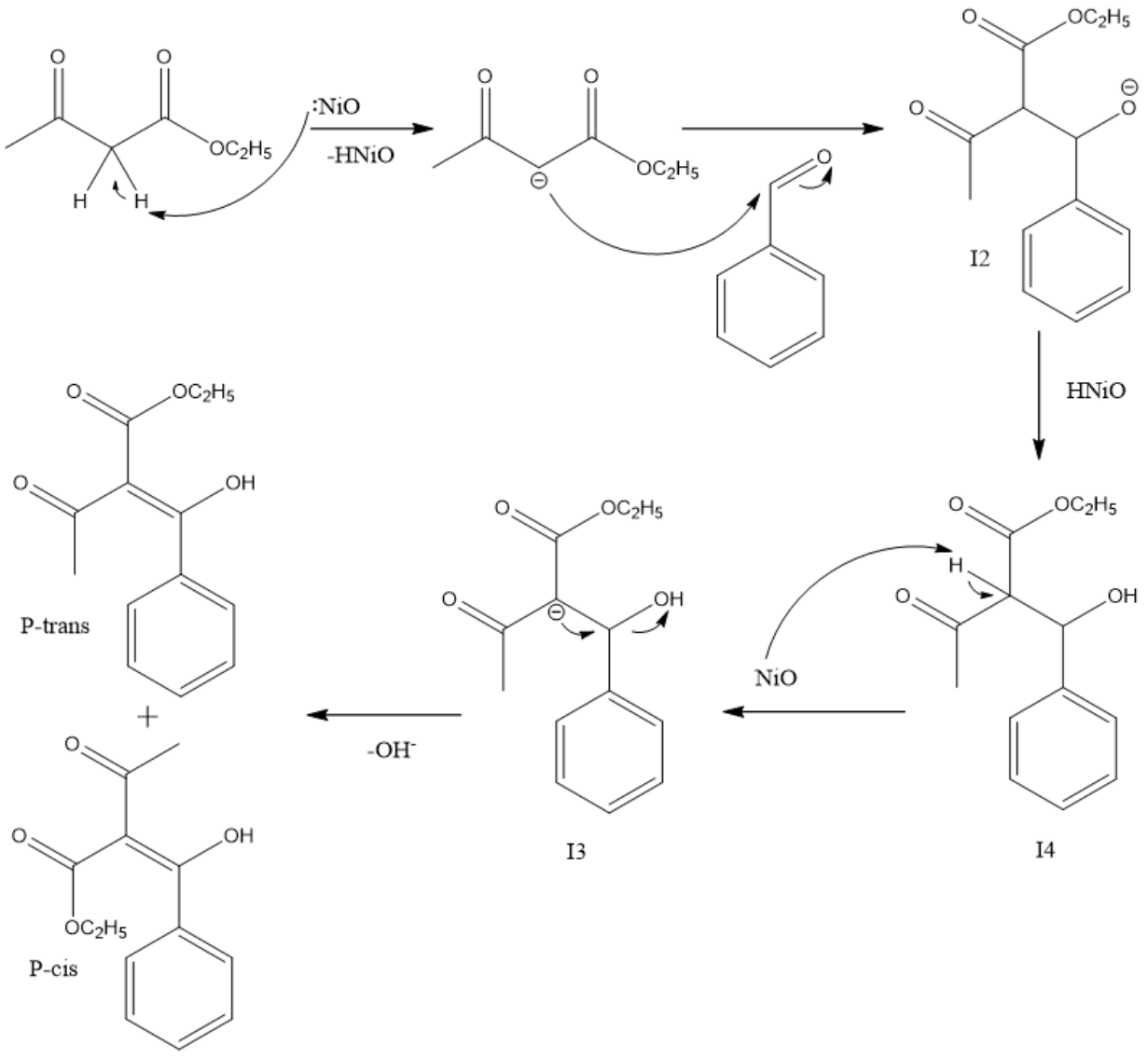

Scheme 4. Reaction mechanism in the presence of the commercial NiO catalyst.

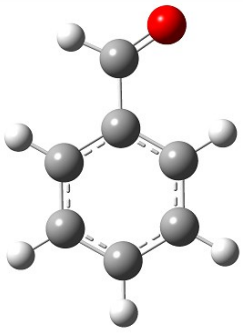

R1

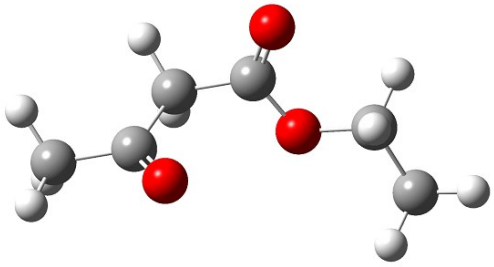

R2

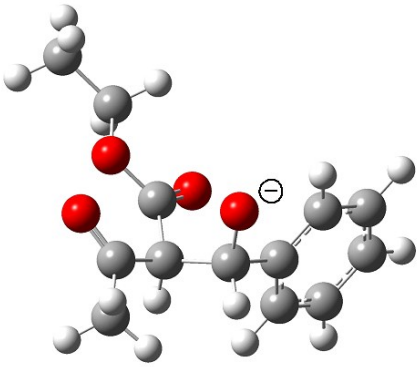

I2

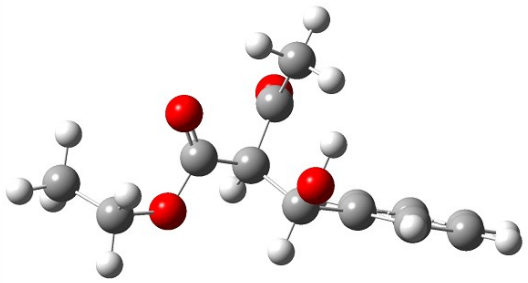

I4

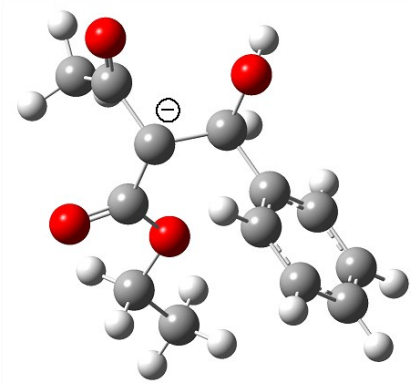

I3

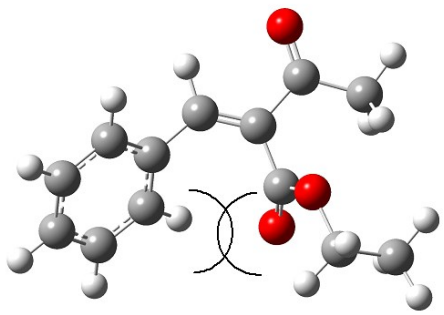

P-cis

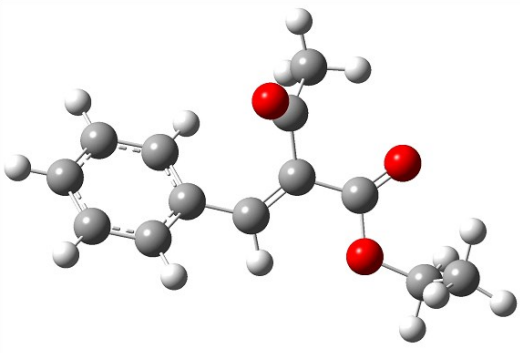

P-trans

Scheme 5. Geometry of reactants and catalyzed intermediates.

4. Conclusion

In the present work, we are interested in the study and the improvement of the optimal conditions of the reaction of Knoevenagel. For this, we have used new basic catalysts, such as commercial NiO, and compared to hydrotalcite NiAl-HT and NiO-HT drived from hydrotalcite which allow a simple, easy and efficient synthesis of the intermediates of the dihydropyridine derivatives which have important pharmaceutical properties. The intermediates of the dihydropyridine derivatives were synthesized from the condensation of benzaldehyde with ethyl acetoacetate without solvent. The catalytic activity is low for the solid NiAl-HT. This low catalytic inertia of this sample is linked to the decrease of its specific surface. After heat treatment of NiO-HT solid the recorded conversion shows a significant improvement which can be explained by the strength the basic sites of the oxides. Furthermore, the conversion rate of commercial NiO is higher than that NiO-HT. The difference of conversion can be justified by the purity and the synthesis under ideal conditions of commercial NiO. The modeling of the Knoevenagel reaction has led to the conclusion that obtaining P-trans in the presence of the catalyst is more favorable than P-cis.

Acknowledgements

This work is supported by the Centre de Recherche Scientifique et Technique en Analyses Physico-Chimiques (CRAPC), Algeria, for the financial support.

CRediT Author Statement

Authors Contributions: **Nadia Aider**: Writing - Original Draft, Visualization, Funding Acquisition, Conceptualization; **Baya Djebarri**: writing – original draft (supporting), Funding acquisition; **Fouzia Touahra**: Supervision (lead), validation (equal), visualization (equal), funding acquisition (equal), review and editing; **Hatem Layeb**: Writing - Original Draft, Formal analysis, Conceptualization; **Djamila Halliche**: Supervision (lead), validation (equal), visualization (equal).

References

[1] Johari, S., Johan, M.R., Khaligh, N.G. (2022). An Overview of Metal-free Sustainable Nitrogen-based Catalytic Knoevenagel Condensation Reaction. *Organic & Biomolecular Chemistry*, 20, 2164-2186. DOI : 10.1039/D2OB00135G

[2] Van Beurden, K., de Koning, S., Molendijk, D., Van Schijndel, J. (2020). The Knoevenagel reaction: a review of the unfinished treasure map to forming carbon–carbon bonds. *Green Chemistry Letters and Reviews*, 13, 349-364. DOI : 10.1080/17518253.2020.1851398

[3] Chakraborty, S., Paul, A.R., Majumdar, S. (2022). Base and metal free true recyclable medium for Knoevenagel condensation reaction in SDS-ionic liquid-aqueous miceller composite system. *Results in Chemistry*, 4, 100294. DOI : 10.1016/j.rechem.2022.100294

[4] Tietze, L.F., Rackelmann, N. (2004). Domino reactions in the synthesis of heterocyclic natural products and analogs. *Pure and Applied-Chemistry*, 76, 1967-1983. DOI : 10.1351/pac200476111967

[5] Dumbre, D.K., Mozammel, T., Selvakannan, P.R., Hamid, S.B.A., Choudhary, V.R., Bhargava, S.K. (2015). Thermally decomposed mesoporous Nickel Iron hydrotalcite: An active solid-base catalyst for solvent-free Knoevenagel condensation. *Journal of Colloid and Interface Science*, 441, 52-58. DOI : 10.1016/j.jcis.2014.11.018

[6] Bartoli, G., Bosco, M., Carlone, A., Dalpozzo, R., Galzerano, P., Melchiorre, P., Sambri, L. (2008). Magnesium perchlorate as efficient Lewis acid for the Knoevenagel condensation between ß-diketones and aldehydes. *Tetrahedron Letters*, 49, 2555-2557. DOI : 10.1016/j.tetlet.2008.02.093

[7] Attanasi, O., Filippone, P., Mei, A. (1983). Effect of metal ions in organic synthesis. Part XVI. Knoevenagel condensations of aldehydes and tosylhydrazones with 2, 4-pentanedione by copper (II) chloride-catalyzed reaction. *Synthetic Communications*, 13, 1203-1208. DOI : 10.1080/00397918308063734.

[8] Narsaiah, A.V., Nagaiah, K. (2003). An efficient knoevenagel condensation catalyzed by $LaCl_3.7H_2O$ in heterogeneous medium. *Synthetic Communications*, 33, 3825-3832. DOI : 10.1081/SCC-120025194.

[9] Rao, P.S., Venkataratnam, R.V. (1991). Zinc chloride as a new catalyst for Knoevenagel condensation. *Tetrahedron Letters*, 32, 5821-5822. DOI : 10.1016/S0040-4039(00)93564-0

[10] Pridgen, L.N., Huang, K., Shilcrat, S., Tickner-Eldridge, A., DeBrosse, C., Haltiwanger, R.C. (1999). An unprecedented asymmetric Nazarov cyclization for the synthesis of non-racemic indanes as endothelin receptor antagonists. *Synlett*, 1999, 1612-1614. DOI : 10.1055/s-1999-2912

[11] Ilangovan, A., Muralidharan, S., Maruthamuthu, S. (2011). A systematic study on Knoevenagel reaction and Nazarov cyclization of less reactive carbonyl compounds using rare earth triflates and its applications. *Journal of the Korean Chemical Society*, 55, 1000-1006. DOI: 10.5012/jkcs.2011.55.6.1000

[12] Dumbre, D.K., Mozammel, T., Selvakannan, P.R., Hamid, S.B.A., Choudhary, V.R., Bhargava, S.K. (2015). Thermally decomposed mesoporous Nickel Iron hydrotalcite: An active solid-base catalyst for solvent-free Knoevenagel condensation. *Journal of Colloid and Interface Science*, 441, 52-58. DOI : 10.1016/j.jcis.2014.11.018

[13] da Silva, J.F., da Silva Ferracine, E.D., Cardoso, D. (2022). Improved accessibility of Na-LTA zeolite catalytic sites for the Knoevenagel condensation reaction. *Microporous and Mesoporous Materials*, 331, 111640. DOI : 10.1016/j.micromeso.2021.111640

[14] Pérez, C.N., Monteiro, J.L.F., López Nieto, J.M., Henriques, C.A. (2009). Influence of basic properties of Mg, Al-mixed oxides on their catalytic activity in knoevenagel condensation between benzaldehyde and phenylsulfonylacetonitrile. *Química Nova*, 32, 2341-2346. DOI: 10.1590/S0100-40422009000900020.

[15] Testa, M.L., La Parola, V. (2021). Sulfonic acid-functionalized inorganic materials as efficient catalysts in various applications: A mini review. *Catalysts*, 11, 1143. DOI : 10.3390/catal11101143

[16] Aider, N., Touahra, F., Bali, F., Djebarri, B., Lerari, D., Bachari, K., Halliche, D. (2018). Improvement of catalytic stability and carbon resistance in the process of CO_2 reforming of methane by CoAl and CoFehydrotalcite-derived catalysts. *International Journal of Hydrogen Energy*, 43, 8256-8266. DOI : 10.1016/j.ijhydene.2018.03.118.

[17] Bouteraa, S., Saiah, F. B. D., Hamouda, S., Bettahar, N. (2020). Zn-M-CO_3 Layered double hydroxides (M= Fe, Cr, or Al): synthesis, characterization, and removal of aqueous indigo carmine. *Bulletin of Chemical Reaction Engineering & Catalysis*, 15(1), 43-54. DOI : 10.9767/bcrec.15.1.5053.43-54

[18] Jiang, Z., Sun, F., Frost, R.L., Ayoko, G., Qian, G., Ruan, X. (2022). Adsorption characteristics of assembled and unassembled Ni/Cr layered double hydroxides towards methyl orange. *Journal of Colloid and Interface Science*, 617, 363-371. DOI : 10.1016/j.jcis.2022.03.022

[19] Djebarri, B., Touahra, F., Aider, N., Bali, F., Sehailia, M., Chebout, R., Halliche, D. (2020). Enhanced Long-term Stability and Carbon Resistance of Ni/Mn_xO_y-Al_2O_3 Catalyst in Near-equilibrium CO_2 Reforming of Methane for Syngas Production. *Bulletin of Chemical Reaction Engineering & Catalysis*, 15, 331-347. DOI : 10.9767/bcrec.15.2.6983.331-347

[20] Cavani, F., Trifiro, F., Vaccari, A. (1991). Hydrotalcite-type anionic clays: Preparation, properties and applications. *Catalysis Today*, 11, 173-301. DOI: 10.1016/0920-5861(91)80068-K

[21] El Khanchaoui, A., Sajieddine, M., Mansori, M., Essoumhi, A. (2022). Anionic dye adsorption on ZnAlhydrotalcite-type and regeneration studies based on "memory effect". *International Journal of Environmental Analytical Chemistry*, 102, 3542-3560. DOI : 10.1080/03067319.2020.1772769

[22] Lu, Y., Jiang, B., Fang, L., Ling, F., Gao, J., Wu, F., Zhang, X. (2016). High performance NiFe layered double hydroxide for methyl orange dye and Cr(VI) adsorption. *Chemosphere*, 152, 415-422. DOI : 10.1016/j.chemosphere.2016.03.015

[23] Touahra, F., Sehailia, M., Halliche, D., Bachari, K., Saadi, A., Cherifi, O. (2016). (MnO/Mn_3O_4)-NiAl nanoparticles as smart carbon resistant catalysts for the production of syngas by means of CO_2 reforming of methane: Advocating the role of concurrent carbothermic redox looping in the elimination of coke. *International Journal of Hydrogen Energy*, 46, 21140-21156. DOI : 10.1016/j.ijhydene.2016.08.194

[24] Devi, R., Begum, P., Bharali, P., Deka, R. C. (2018). Comparative study of potassium salt-loaded MgAlhydrotalcites for the Knoevenagel condensation reaction. *ACS Omega*, 3, 7086-7095. DOI : 10.1021/acsomega.8b00767

[25] Mancipe, S., Castillo, J.C., Brijaldo, M.H., López, V.P., Rojas, H., Macías, M.A., Luque, R. (2022). B-Containing Hydrotalcites Effectively Catalyzed Synthesis of 3-(Furan-2-yl) acrylonitrile Derivatives via the Knoevenagel Condensation. *ACS Sustainable Chemistry & Engineering*, 10, 12602-12612. DOI : 10.1021/acssuschemeng.2c03209

[26] Jadhav, A.L., Yadav, G.D. (2019). Clean synthesis of benzylidenemalononitrile by Knoevenagel condensation of benzaldehyde and malononitrile: effect of combustion fuel on activity and selectivity of Ti-hydrotalcite and Zn-hydrotalcite catalysts. *Journal of Chemical Sciences*, 131, 1-14. DOI : 10.1007/s12039-019-1641-6

[27] Vaccari, A. (1998). Preparation and catalytic properties of cationic and anionic clays. *Catalysis Today*, 41, 53-71. DOI : 10.1016/S0920-5861(98)00038-8

[28] Tichit, D., Coq, B., Cerneaux, S., Durand, R. (2002). Condensation of aldehydes for environmentally friendly synthesis of 2-methyl-3-phenyl-propanal by heterogeneous catalysis. *Catalysis Today*, 75, 197-202. DOI : 10.1016/S0920-5861(02)00069-X

[29] Veloso, C.O., Pérez, C.N., de Souza, B.M., Lima, E.C., Dias, A.G., Monteiro, J.L.F., Henriques, C.A. (2008). Condensation of glyceraldehyde acetonide with ethyl acetoacetate over Mg, Al-mixed oxides derived from hydrotalcites. *Microporous and Mesoporous Materials*, 107, 23-30. DOI : 10.1016/j.micromeso.2007.05.036

[30] Palapa, N.R., Siregar, P.M.S.B.N., Wijaya, A., Taher, T., Lesbani, A. (2022). High Selectivity and Stability Structure of Layered Double Hydroxide-Biochar for Removal Cd(II). *Bulletin of Chemical Reaction Engineering & Catalysis*, 17, 520-532. DOI : 10.9767/bcrec.17.3.14288.520-532.

[31] Mokhtar, M., Saleh, T.S., Basahel, S.N. (2012). Mg–Al hydrotalcites as efficient catalysts for aza-Michael addition reaction: A green protocol. *Journal of Molecular Catalysis A: Chemical*, 353, 122-131. DOI : 10.1016/j.molcata.2011.11.015

[32] Pérez, C.N., Pérez, C.A., Henriques, C.A., Monteiro, J.L.F. (2004). Hydrotalcites as precursors for Mg, Al-mixed oxides used as catalysts on the aldol condensation of citral with acetone. *Applied Catalysis A: General*, 272, 229-240. DOI : 10.1016/j.apcata.2004.05.045

[33] Aider, N., Smuszkiewicz, A., Pérez-Mayoral, E., Soriano, E., Martín-Aranda, R.M., Halliche, D., Menad, S. (2014). Amino-grafted SBA-15 material as dual acid–base catalyst for the synthesis of coumarin derivatives. *Catalysis Today*, 227, 215-222. DOI: 10.1016/j.cattod.2013.10.016

[34] Majumdar, K.C., Taher, A., Ray, K. (2009). Domino-Knoevenagel-hetero-Diels–Alder reactions: an efficient one-step synthesis of indole-annulated thiopyranobenzopyran derivatives. *Tetrahedron Letters*, 50, 3889-3891. DOI : 10.1016/j.tetlet.2009.04.054

[35] Gu, X., Tang, Y., Zhang, X., Luo, Z., Lu, H. (2016). Organocatalytic Knoevenagel condensation by chiral C2-symmetric tertiary diamines. *New Journal of Chemistry*, 40, 6580-6583. DOI : 10.1039/C6NJ00613B

[36] Sani, A., Hassan, D., Khalil, A.T., Mughal, A., El-Mallul, A., Ayaz, M., Maaza, M. (2021). Floral extracts-mediated green synthesis of NiO nanoparticles and their diverse pharmacological evaluations. *Journal of Biomolecular Structure and Dynamics*, 39, 4133-4147. DOI : 10.1080/07391102.2020.1775120

[37] Baranwal, K., Dwivedi, L.M., Siddique, S., Tiwari, S., Singh, V. (2021). Chitosan Grown Copper Doped Nickel Oxide Nanoparticles: An Excellent Catalyst for Reduction of Nitroarenes. *Journal of Cluster Science*, 32, 937-947. DOI : 10.1007/s10876-020-01861-0

[38] Aoudjit, L., Halliche, D., Bachari, K., Saadi, A., Cherifi, O. (2017). Nickel-containing mesoporous silicas as a catalyst for the Pechmann condensation reaction. *Theoretical and Experimental Chemistry*, 53, 112-121. DOI : 10.1007/s11237-017-9507-9

[39] Becke, A.D. (1993). Density-Functional Thermochemistry. III. The Role of Exact Exchange. *The Journal of Chemical Physics*, 98, 5648-5652. DOI : 10.1063/1.46491

[40] Lee, C., Yang, W., Parr, R.G. (1988). Development of the Colle-Salvetti correlation-energy formula into a functional of the electron density. *Physical Review B*, 37(2), 785. DOI : 10.1103/PhysRevB.37.785

[41] Hehre, W.J., Radom, L., Schleyer, P.v.R., People, J. (1986). *Ab initio Molecular Orbital Theory*. John Wiley and Sons.

[42] Morioka, K., Asami, Y., Tanaka, K., ONO, T., Saheki, S., Harada-Saheki, K., Tanaka, T. (1980). Isozyme patterns of pyruvate kinase and differentiation of Friend leukemia cells. *GANN Japanese Journal of Cancer Research*, 71, 146-150. DOI : 10.20772/cancersci1959.71.1_146

[43] Schlegel, H.B. (1995). Geometry optimization on potential energy surfaces. In Yarkony, D.R. (Ed.) *Modern Electronic Structure Theory: Part I,* pp. 459-500. DOI : 10.1142/9789812832108_0008

[44] Frisch, M.J.; Trucks, G.W., Schlegel, H.B., Scuseria, G.E., Robb, M.A., Cheeseman, J. R. *et al*., Gaussian, Inc., Wallingford CT, 2016.

[45] Makri, M.M., Vasiliades, M.A., Petallidou, K.C., Efstathiou, A.M. (2016). Effect of support composition on the origin and reactivity of carbon formed during dry reforming of methane over 5wt% Ni/$Ce_{1-x}M_xO_{2-\delta}$ (M= Zr^{4+}, Pr^{3+}) catalysts. *Catalysis Today*, 259, 150-164. DOI : 10.1016/j.cattod.2015.06.010

[46] Mette, K., Kühl, S., Tarasov, A., Willinger, M. G., Kröhnert, J., Wrabetz, S., Lunkenbein, T. (2016). High-temperature stable Ni nanoparticles for the dry reforming of methane. *ACS Catalysis*, 6, 7238-7248. DOI : 10.1021/acscatal.6b01683

[47] Braterman, P.S., Xu, Z.P., Yarberry, F. (2004). Layered double hydroxides (LDHs). *Handbook of Layered Materials*, 8, 373-474. DOI : 10.1201/9780203021354.ch8

[48] Djebarri, B., Gonzalez-Delacruz, V.M., Halliche, D., Bachari, K., Saadi, A., Caballero, A., Cherifi, O. (2014). Promoting effect of Ce and Mg cations in Ni/Al catalysts prepared from hydrotalcites for the dry reforming of methane. *Reaction Kinetics, Mechanisms and Catalysis*, 111, 259-275. DOI : 10.1007/s11144-013-0646-2

[49] Rivera, J.A., Fetter, G., Jiménez, Y., Xochipa, M.M., Bosch, P. (2007). Nickel distribution in (Ni,Mg)/Al-layered double hydroxides. *Applied Catalysis A: General*, 316(2), 207-211. DOI : 10.1016/j.apcata.2006.09.031

[50] Kloprogge, J.T., Wharton, D., Hickey, L., Frost, R.L. (2002). Infrared and Raman study of interlayer anions CO_3^{2-}, NO_3^-, SO_4^{2-} and ClO_4^- in Mg/Al-hydrotalcite. *American Mineralogist*, 87, 623-629. DOI : 10.2138/am-2002-5-604

[51] Occelli, M.L., Olivier, J.P., Auroux, A., Kalwei, M., Eckert, H. (2003). Basicity and porosity of a calcined hydrotalcite-type material from nitrogen porosimetry and adsorption microcalorimetry methods. *Chemistry of Materials*, 15, 4231-4238. DOI : 10.1021/cm030105b

[52] Khairnar, S.D., Shrivastava, V.S. (2019). Facile synthesis of nickel oxide nanoparticles for the degradation of Methylene blue and Rhodamine B dye: a comparative study. *Journal of Taibah University for Science*, 13, 1108-1118. DOI : 10.1080/16583655.2019.1686248

[53] Chmielarz, L., Kuśtrowski, P., Rafalska-Łasocha, A., Dziembaj, R. (2002). Influence of Cu, Co and Ni cations incorporated in brucite-type layers on thermal behaviour of hydrotalcites and reducibility of the derived mixed oxide systems. *Thermochimica Acta*, 395, 225-236. DOI : 10.1016/S0040-6031(02)00214-9

[54] Beach, E.R., Shqau, K., Brown, S.E., Rozeveld, S.J., Morris, P.A. (2009). Solvothermal synthesis of crystalline nickel oxide nanoparticles. *Materials Chemistry and Physics*, 115, 371-377. DOI : 10.1016/j.matchemphys.2008.12.018

[55] Chaudhary, R.G., Tanna, J.A., Mondal, A., Gandhare, N.V., Juneja, H.D. (2017). Silica-coated nickel oxide a core-shell nanostructure: synthesis, characterization and its catalytic property in one-pot synthesis of malononitrile derivative. *Journal of the Chinese Advanced Materials Society*, 5, 103-117. DOI : 10.1080/22243682.2017.1296371

[56] Perozo-Rondon, E., Calvino-Casilda, V., Martín-Aranda, R.M., Casal, B., Duran-Valle, C.J., Rojas-Cervantes, M.L. (2006). Catalysis by basic carbons: Preparation of dihydropyridines. *Applied Surface Science*, 252, 6080-6083. DOI : 10.1016/j.apsusc.2005.11.017

[57] Lett, J.A., Sagadevan, S., Weldegebrieal, G. K., Fatimah, I. (2022). Hydrothermal synthesis and photocatalytic activity of NiO nanoparticles under visible light illumination. *Bulletin of Chemical Reaction Engineering & Catalysis*, 17, 340-349. DOI : 10.9767/bcrec.17.2.13680.340-349